JOURNAL OF AGRICULTURAL AND FOOD CHEMISTRY

Treatment of Mcf-7 Breast Cancer Cells with a Red Grape Wine Polyphenol Fraction Results in Disruption of Calcium Homeostasis and Cell Cycle Arrest Causing Selective Cytotoxicity

FATIMA HAKIMUDDIN,[†] GOPINADHAN PALIYATH,*[,†,‡] AND KELLY MECKLING[§]

Department of Food Science, Department of Plant Agriculture, and Department of Human Health and Nutritional Sciences, University of Guelph, Guelph, Ontario N1G 2W1, Canada

Food components influence the physiology by modulating gene expression and biochemical pathways within the human body. The disease-preventive roles of several fruit and vegetable components have been related to such properties. Polyphenolic components such as flavonoids are strong antioxidants and induce the expression of several xenobiotic-detoxifying enzymes. The mechanism of selective cytotoxicity induced by red grape wine polyphenols against MCF-7 breast cancer cells was investigated in relation to their interference with calcium homeostasis. MCF-7 cells showed an increase in cytosolic calcium levels within 10 min of treatment with the polyphenols. Immunohistochemical localization of calmodulin with secondary gold-labeled antibodies showed similar levels of gold labeling in both MCF-7 cells and the spontaneously immortalized, normal MCF-10A cell line. MCF-7 cells treated with the red wine polyphenol fraction (RWPF) showed swelling of endoplasmic reticulum, dissolution of the nucleus, and loss of plasma membrane integrity as well as reduced mitochondrial membrane potential. These cells were arrested at the G2/M interphase. By contrast, MCF-10A cells did not show such changes after RWPF treatment. The results suggest that polyphenol-induced calcium release may disrupt mitochondrial function and cause membrane damage, resulting in selective cytotoxicity toward MCF-7 cells. This property could further be developed toward breast cancer prevention strategies either independently or in conjunction with conventional prevention therapies where a positive drug−nutrient interaction can be demonstrated.

KEYWORDS: Calmodulin; calcium signaling; cell cycle arrest; diet and cancer; red wine polyphenols

INTRODUCTION

Breast cancer is the most common form afflicting females in Western countries and the second leading cause of cancer-related deaths among North American women (*1*). Major emphasis has been placed on understanding the role of genetic, hormonal, environmental, and dietary factors that influence the risk of developing breast cancer. A large body of epidemiological evidence, together with data from animal and in vitro studies, strongly supports the cancer-preventive properties of several dietary constituents. In general, vegetables and fruits, dietary fiber, and certain micronutrients appear to be protective against cancer (*2*), whereas fat, excessive calories, and alcohol seem to increase the risk of developing cancer (*3*). However, the data gathered from different studies are not consistent and may result from several contributing factors such as inherited genetic susceptibility among individuals and diverse lifestyle behavior (*4*). In this context, a recent study showed that dietary risk factors for colorectal cancer are associated with p53 subtypes. Cruciferous vegetables may be protective for colorectal cancer development through a p53-dependent pathway, whereas beef consumption may increase the risk for colorectal cancer through a p53-independent pathway (*5*).

Signal transduction pathways regulate numerous cell processes including growth, proliferation, and death. Defective signal transduction is often associated with aberrant cell cycle regulation, which in turn can lead to the development and progression of cancer. Several signal transduction pathways such as the Erk/MAP kinase pathway and the PI 3-kinase pathway have been implicated in mammary carcinogenesis, through their uncontrolled activation (*6*). The central role of Ca^{2+} as an intracellular signal involved in cell proliferation has been widely examined (*7*, *8*). Calcium and calcium-binding proteins such as calmodulin have an active role in the regulation of cell cycle in normal and aberrant cell proliferation and in apoptotic cell death. The role of calmodulin in triggering DNA replication has been clearly demonstrated by experiments using anti-calmodulin drugs such as trifluoperazine, W7, and W13 that

* Corresponding author. Phone: 519-824-4120, ext 54856. Fax: 519-767-0755. E-mail: gpaliyat@uoguelph.ca.
[†] Department of Food Science.
[‡] Department of Plant Agriculture.
[§] Department of Human Health and Nutritional Sciences.

10.1021/jf060834m CCC: $33.50
Published on Web 09/06/2006

inhibited DNA replication (*9*). As well, transfection with the calmodulin gene in the sense or antisense direction in C127 mice, respectively, lengthened or shortened the G1 phase of the cell cycle (*10*). However, calcium/calmodulin-regulated steps involved in the triggering of DNA synthesis still remain unclear.

Vegetables and fruits contain a wide variety of phytochemicals such as terpenes, polyphenols, carotenoids, and sulfur-containing compounds that have the potential to reduce cancer development. The specific mechanisms of cancer-preventive action of these phytochemicals are being unravelled in several studies (*11*). Polyphenols present in several foods and beverages are known for their antioxidant and cancer chemopreventive properties. Resveratrol, a polyphenol found in grapes and wine induces phase II enzymes and inhibits I kappa B kinase activity, the key regulator of NF-kappa B activation, and signalling enzymes such as protein kinase C in U-937 myeloid and HeLa and H4 epithelial cells (*12*). Sulforaphane, a cancer chemopreventive agent found in cruciferous vegetables such as broccoli, induces apoptosis in SV-40-transformed mouse embryonic fibroblasts through the activation of Bcl-2 family of proteins Bax and Bak, which in turn are translocated to mitochondria causing the release of apoptogenic molecules such as cytochrome *c* into the cytosol (*13*).

Among common foods, red wine contains a variety of polyphenols that have shown promising cancer-preventive and therapeutic activity due to their effects on multiple targets at levels comparable to those found in human plasma (*14*). Though it was initially hypothesized that the biological effects of polyphenols are related to their antioxidant activity, available evidence from cell culture experiments suggests that many of the biological effects of polyphenols are related to their ability to modulate cell-signalling pathways (*15*). In our previous studies (*16*), we demonstrated that specific polyphenol fractions from red grape wine showed selective cytotoxicity toward MCF-7 breast cancer cells, as compared to the non-tumorigenic MCF-10A cells and normal human mammary epithelial cells (HMEC). By contrast, authentic flavonoids such as quercetin and naringenin were more toxic to HMEC than cancer cells. The cell growth inhibitory activity of red wine polyphenols also correlated with their calmodulin antagonistic activity. This suggested a possible relationship between the inhibition of calcium−calmodulin second messenger system and inhibition of breast cancer development. In this study, we have attempted to delineate the mechanism of anti-proliferative action of the red wine polyphenols in relation to their effect on calcium−calmodulin signalling systems and other calcium-mediated processes such as mitochondrial function and cell cycle progression in malignant (MCF-7) and normal (MCF-10A) human mammary epithelial cells.

MATERIALS AND METHODS

Cell Lines and Culture Conditions. An estrogen-receptor positive human breast cancer cell line (MCF-7) was obtained from American Tissue type Culture Collection (ATCC, Bethesda, MD). The MCF-7 breast cancer cells were cultured in α-minimum essential medium. The medium was supplemented with 10% fetal bovine serum, 1 mM sodium pyruvate, 100 U/mL penicillin, 100 ng/mL streptomycin, and 10 μg/mL insulin.

A spontaneously immortalized human breast epithelial cell line (MCF-10A) obtained from ATCC (Bethesda, MD) was cultured in 50:50 Dulbecco's modified eagle's medium: HAM's F12 nutrient mixture supplemented with 5% horse serum, 10 μg/mL insulin, 0.5 μg/mL hydrocortisone, 20 ng/mL epidermal growth factor, and 100 ng/mL choleratoxin. (MCF-10A cells are naturally immortalized, normal epithelial cells of mammary origin that do not produce tumors in athymic animals.)

Table 1. Anthocyanin and Polyphenol Composition of 60–80% Wine Fraction[a]

component	amount (nmol/100 μg of phenols)
delphinidin-3-*O*-glucoside	trace
cyanidin-3-*O*-glucoside	ND
petunidin-3-*O*-glucoside	trace
peonidin-3-*O*-glucoside	ND
malvidin-3-*O*-glucoside	trace
delphinidin-3-*O*-acetoyl glucoside	7.04 (3.57)
cyanidin-3-*O*-acetoyl glucoside	trace
petunidin-3-*O*-acetoyl glucoside	9.22 (4.81)
malvidin-3-*O*-acetoyl glucoside	25.22 (13.5)
petunidin-3-*O*-acetoyl glucoside derivative	24.18 (17.1)
delphinidin-3-(6′-coumaroyl) glucoside	18.20 (11.1)
petunidin-3-(6′-coumaroyl) glucoside	39.44 (24.6)
malvidin-3-(6′-coumaroyl) glucoside	32.72 (20.9)
unidentified	5.00 (4.25)
O-methyl quercetin	1.00 (0.32)
myricetin	trace
kaempferol	trace
catechin glycoside	trace
epicatechin glycoside	trace
O-methyl resveratrol	trace

[a] ND, not detectable; traces, <0.1 nmol/100 μg of phenols. Values in parentheses indicate the amount in μg/100 μg of polyphenols.

Cell lines were grown at 37 °C in a humidified atmosphere supplemented with 5% CO_2 and 95% air and maintained by transfer into fresh medium at appropriate intervals. Growth, division, and morphology of the cells were monitored periodically.

Isolation of Red Grape Wine Polyphenol Fraction (RWPF). Different methanolic fractions of polyphenols were obtained from merlot red wine by fractionation on Sep-Pak C_{18} columns (Waters) using methanol−water mixtures of various proportions according to the method previously described (*16*). The polyphenol fractions eluted by 60% v/v and 80% v/v methanol, were selectively cytotoxic to MCF-7 breast cancer cells by comparison to authentic flavonoids such as quercetin, catechin, and naringenin, which were relatively more cytotoxic to normal cells. HPLC−MS analysis of the 60−80% pooled fraction revealed the presence of several anthocyanins. The composition of anthocyanins that make up the 60−80% fraction is given in **Table 1**. This fraction was low in anthocyanin glycosides such as delphinidin-3-*O*-glucoside, cyanidin-3-*O*-glucoside, petunidin-3-*O*-glucoside, peonidin-3-*O*-glucoside, and malvidin-3-*O*-glucoside, some of which were detectable only in traces. However, this fraction was enriched in the relatively hydrophobic anthocyanins that include the acetoyl and coumaroyl derivatives of delphinidin, petunidin, and malvidin. In addition, smaller amounts (<0.1 nmol/100 μg of phenols) of flavonoid aglycones such as *O*-methyl quercetin, myricetin, kaempferol, and the flavan-3-ols catechin and epicatechin glycosides as well as the stilbene alcohol *O*-methyl resveratrol were detected by GC−MS analysis. The 60−80% fraction accounted for 316 mg of 1489 mg of total polyphenols recovered from the column (the rest constituted by 980 mg eluted by 40% methanol and the flow through that was equivalent to nearly 200 mg) present in a liter of red wine (*16*). For convenience, the combined fraction eluted by 60% and 80% methanol is referred to as RWPF hereafter. Aliquots of RWPF were stored at −20 °C until further use.

Calmodulin (CaM) Activity. Calmodulin activity was assayed by using its property of stimulating activator-deficient cAMP phosphodiesterase (3′,5′-cyclic nucleotide 5′-nucleotidohydrolase, EC 3.1.4.17, which converts cAMP to 5′AMP) from bovine heart (*17*). The assay was conducted in a medium containing 40 mM Tris-HCl, pH 7.0, 1 mM $CaCl_2$, 0.4 mM $MnCl_2$, and 1 mM cAMP. Phosphodiesterase was used at a concentration of 0.02 U/mL and calmodulin (bovine brain) at 2 U/mL. CaM was also extracted and purified from untreated and RWPF-treated (50 μg/mL) MCF-7 cells by passing the cell lysate sequentially through PD10 (desalting columns) and phenyl-sepharose affinity columns (Sigma Chemical Co., St. Louis, MO). CaM bound to the affinity column was eluted with 2 mM EGTA (*18*). Samples

were dialyzed against 10 mM Tris buffer, pH 8; freeze-dried; and dissolved in 10 mM Tris buffer before using them for activity assays. An aliquot containing around 60 μg of total protein was added to the calmodulin assay mixture, which was adjusted to a final volume of 500 μL with water and incubated at 25 °C for 30 min. The reaction was stopped by heating in a boiling water bath. The 5′-AMP formed from cAMP was separated and quantified by using a X-Terra RP_{18} column (3.9 × 150 mm, Waters Corporation, Milford, MA) at ambient conditions. The mobile phase was 10 mM KH_2PO_4, pH 2.5, delivered at 1.5 mL/min by a Waters 626 pump. The elution of 5′-AMP and cAMP was monitored by absorbance at 260 nm using a Waters 486 absorbance detector. Peak areas were a linear function of 5′-AMP concentration up to 1.7 μg in the absorbance mode.

Total Protein Extraction. MCF-7 and MCF-10A cells were synchronized by double thymidine block and treated with 50 μg/mL RWPF for 30 min, 6 h, 12 h, and 24 h. Cells were harvested, washed, suspended in lysis buffer [50 mM HEPES, 5 mM EDTA, 2 mM EGTA, 1 mM DTT, 1 tablet of the protease inhibitor cocktail/10 mL (Boerhinger-Mannheim)] and sonicated for 30 s. Protein concentrations of the cell lysates were quantified by the protein-dye binding method (*19*).

Western Blotting for Calmodulin. Cell lysates containing 50−100 μg of total protein were denatured by heating in a boiling water bath using 2 × SDS/sample buffer 1:1 [25 mL of 4× Tris-HCl/SDS (pH 6.8), 20 mL of glycerol, 4 g of SDS, 3.1 g of DTT, 1 mg of bromophenol blue, and water to a final volume of 100 mL] and 50 μg of protein/lane were loaded on SDS−polyacrylamide gels (SDS−PAGE, 4% stacking/12% running gel) and subjected to electrophoresis at 30 mA current until the dye front reached the bottom of the gel. Proteins were transferred on to PVDF membranes using a Bio-Rad trans-blot apparatus for 2 h at 350 mA in KP buffer (25 mM KH_2PO_4/K_2HPO_4 buffer, pH 7.0). Membranes were fixed in KP buffer with 0.2% glutaraldehyde for 45 min, rinsed with KP buffer, and blocked in 3% gelatin in Tris-buffered saline (TBS, 20 mM Tris, 500 mM NaCl, pH 7.5) at 37 °C for 1 h. Membranes were later washed with TBS for 10 min and incubated in antibody buffer [1% gelatin−TTBS (20 mM Tris, 500 mM NaCl, 0.05% Tween-20, pH 7.5)] containing the primary antibody (monoclonal mouse anti-CaM, Sigma Chemical Co, St. Louis, MO) overnight at 4 °C at a dilution of 1:1000. After washing 2× 8 min each in TTBS and 1× 8 min in TBS, the membrane was incubated at 30 °C with shaking in goat anti-mouse secondary antibody (3.3 μL in 10 mL of antibody buffer) coupled to alkaline phosphatase (AP) (Bio-Rad Corp., Mississauga, ON) for 1 h. After the wash, 2× in TTBS (8 min) and 1× in TBS (8 min), membranes were developed in a solution containing 0.5 mL of AP color reagent A, 0.5 mL of AP color reagent B, and 50 mL of 1× AP color development buffer at room temperature. Finally, membranes were washed in distilled water for 10 min with gentle agitation, dried on filter paper, and stored between polyester sheets, protected from light.

Immunolocalization of Calmodulin. MCF-7 and MCF-10A cells were cultured and treated with the IC_{50} concentration of RWPF (50 μg/mL) at the desired time intervals. Briefly, the cells were harvested from the flasks by 0.5% Trypsin/EDTA, washed with phosphate-buffered saline (PBS) containing 5 mM EDTA and 2 mM EGTA, sedimented by gentle centrifugation (1000*g*) in a bench top centrifuge, and fixed in a mixture of 4% paraformaldehyde and 0.5% glutaraldehyde for a minimum of 1 h. The fixed cells were dehydrated through a graded series of 50%, 70%, 90%, and 95% ethanol and infiltrated into K4M resin. Ultrathin sections were cut and picked up on Fomvar-coated nickel grids. The immunolabeling procedure was as follows: sections were incubated with 0.05 M glycine in PBS for 15 min to inactivate residual aldehyde groups present after aldehyde fixation. To block nonspecific binding sites, sections were then incubated in PBS buffer with 5% BSA and 0.1% corn water fish skin gelatin supplemented with 5% normal mouse serum for 30 min. After being washed with incubation buffer for 5 min, sections were labeled with primary antibody (1:10) overnight at 4 °C. A second wash in incubation buffer was done 3× 5 min each, after which sections were incubated with the secondary antibody−gold conjugate (25 nm gold particles coupled to goat anti-mouse antibody; Electron Microscopy Sciences, NJ) diluted 1:20 in incubation buffer for 2 h at room temperature. Final washes were performed in incubation buffer 3× and ultrapure water 4×, and sections were blot dried and examined using a transmission electron microscope (Leo 912 B).

Measurement of Intracellular Calcium. Cells were plated to a concentration of 2 × 10^5 cells in 60 mm petri dishes and grown for 24−48 h. The plates were washed with PBS, and cells were loaded with 10 μM Calcium Green-2 AM ester (5 μM, Molecular Probes, Eugene, OR) in α-MEM (modified Eagle's medium) without FBS. Pluronic F-127 (0.2%, Molecular Probes), a mild detergent, was added to facilitate uniform loading of the cells with the dye. Plates were incubated for 30 min at 37 °C. After loading, cells were washed with PBS (to remove nonspecifically associated dye) and MEM. Plates were incubated for 10−15 min at room temperature. The cells were treated with 50 μg/mL RWPF after recording the basal image. Fluorescence microscopy was performed with a Leica Spectral Confocal and Multiphoton System (Leica Microsystems) equipped with suitable filter packs that allowed the specimens to be excited at specific wavelengths. A personal computer with Leica Confocal Software LCS 2.5.1227 was attached to the microscope for image acquisition and analysis.

The fluorescence was monitored at excitation 503 nm/emission 536 nm. Calcium Green-2 is sensitive to calcium concentration changes in the range of 0.01−500 μM. However, because of the limitations of the microscope system, the sensitivity range in our experiments was between 0.01 and 0.6 μM (calcium concentration-fluorescence values were 0 calcium, 3; 0.017 μM, 39; 0.038 μM, 50; 0.065 μM, 75; 0.225 μM, 188; 0.602 μM, 255; 1.35 μM, 256). Calibration for calcium concentration and fluorescence emission was conducted in cavity slides using various concentrations of calcium. The fluorescence emission was calibrated against calcium concentration by using Ca-EGTA/K-EGTA premixed solution provided in the kit using standard procedures (calcium calibration kit, Molecular Probes).

Evaluation of Mitochondrial Membrane Potential. Alterations in the mitochondrial membrane potential were analyzed by confocal laser scanning microscopy using the mitochondrial potential-sensitive dye JC-1 (5,5′6,6′-tetrachloro-1,1,3,3′-tetraethylbenzimidazolcarbocyanine iodide; Molecular Probes, Eugene, OR). Approximately 2 × 10^5 cells were grown in 60 mm plates for 24 h. Cells were later washed once in PBS, resuspended in MEM without phenol red, and incubated with 1 μM JC-1 at 37 °C for 10 min. Stained cells were then washed once in PBS and treated with RWPF (50 μg/mL) for 1−2 h after which the media was replaced with warm PBS (37 °C) and viewed immediately in a confocal microscope. The dye is membrane potential sensitive and accumulates as red fluorescent aggregates in the mitochondria with a high potential and having absorption/ emission maxima of 585/590 nm. In the cytoplasm, JC-1 remains in the green fluorescent monomeric form with absorption/emission maxima of 510/527 nm, when the mitochondrial membrane potential is low. A transition from the red to green fluorescing cells indicates a loss in mitochondrial membrane potential.

Caspase Activity. Cells were plated in 100 mm plates to a concentration of 1 × 10^6 cells. One of the plates was treated with RWPF (50 μg/mL) for 24 h, and the other plate was left untreated. Floating and attached cells were collected from both plates, centrifuged, and washed with cold PBS twice. Cells were pelleted, resuspended in cell lysis buffer, and incubated on ice for 10−15 min. Samples were sonicated, and protein content was measured by Bradford assay. To test for caspase activity, 178 μL of reaction buffer, 30 μL of cell lysate containing 100 μg of total protein and 2 μL of flurogenic caspase substrate conjugated to rhodamine 110, bis-(*N*-CBZ-L-isoleucyl-L-threonyl-L-aspartic acid amide) (Z-IETD-R110; Molecular Probes) were added to a 96-well plate and incubated at room temperature for about 10 min. The release of rhodamine due to caspase activity was monitored at excitation 496 nm and emission 520 nm by a Fluorstar microplate reader for a period of 30 min.

DNA Laddering. MCF-7 cells were plated at 1.0 × 10^6 cells per 100 mm^2 dish. Cells were allowed to recover for 5−6 h and were then treated with RWPF (50 μg/mL) for 3, 6, 12, and 24 h. Cells were washed once with PBS, harvested with trypsin-EDTA, and pelleted at 1000*g* for 10 min. To assess oligonucleosomal fragmentation, the pellet was further processed for genomic DNA extraction using an apoptosis DNA laddering kit (Cayman Chemical Company, Ann Arbor, MI). The

DNA sample was mixed with gel loading buffer and applied to a 1% agarose gel. The gel was run in Tris−acetate−EDTA (TAE; 0.4 M Tris. 10 mM EDTA, 10.9 mL of glacial acetic acid, pH 8.5) buffer at 45 V at RT for approximately 2−3 h, stained with ethidium bromide, and visualized on a UV transilluminator.

Determination of Red−Green Transition in Acridine Orange Stained Cells. MCF-7 and MCF-10A cells were plated at 0.5×10^6 cells per 60 mm dish. Cells were allowed to recover for 5−6 h and were then treated with RWPF at a concentration of 50 μg/mL for 24 h. Cells were washed once with PBS and loaded with 2.5 μg/mL acridine orange (Molecular Probes) in phenol red-free media and incubated for 10−15 min. After being washed with PBS, cells were observed in a confocal laser scanning microscope (Leica Microsystems) under 488 nm illumination by argon laser beam. In acridine orange stained cells, the cytoplasm and nucleolus fluoresce bright green and dim red, respectively, whereas acidic compartments fluoresce bright red where the dye becomes protonated and compartmentalized. Thus, the intensity of the red fluorescence is an indication of the degree of acidity and/or the volume of their cellular acidic compartment. The red (>650 nm) to green (505−545 nm) fluorescence transitions were compared within control and RWPF-treated MCF-7 and MCF-10A cells.

Cell Cycle Distribution Analysis. Cells at 60−70% confluence were treated with RWPF at concentrations near their IC_{50} (50 g/mL) values. Floating and attached cells were collected after 48 h, washed, and resuspended at a density of 1×10^6/mL in PBS + 2% FBS. Three milliliter of 70% ethanol (−20 °C) was pipetted slowly into this suspension while vortexing at top speed. Cells were left in ethanol at 4 °C for at least 1 h. Cells were then pelleted by centrifugation, washed twice in PBS, resuspended in 1 mL of PBS, and incubated in 20 μg of DNase-free RNase at 37 °C for 30 min. Cells were incubated with 10 μg/mL propidium iodide (Molecular Probes) solution in 3.8 mM sodium citrate at room temperature for 10 min. Samples were stored in ice until analysis. Cells were analyzed by a Coulter Elite flow cytometer, gated on forward light scatter, using a dichroic and a band-pass filter and 488 nm argon laser.

Statistical Analysis. All statistical analyses were performed using GraphPad Prism Version 4.02 software.

RESULTS

Effect of RWPF on Cytosolic Calcium Levels. Changes in cytosolic calcium concentrations in MCF-7 and MCF-10A cells were measured using the dye Calcium Green-2 as the Ca^{2+} probe. Optimal sensitivity of detection of calcium concentration by Calcium Green-2 was in the range of 10−600 nM. MCF-7 and MCF-10A cells were preloaded with Calcium Green-2 AM ester and cytosolic calcium levels estimated using a laser confocal microscope. **Figure 1A** shows images of Calcium Green-2-loaded MCF-7 cells taken at 4 min intervals after treatment with 50μg/mL of RWPF, for a period of 30 min. Basal fluorescence level in most of the cells varied between 20−60 units, which corresponded to the resting cytosolic calcium levels of 25−150 nM (**Figure 1C**). A few cells, however, showed a high level of fluorescence (120−160 units) that corresponded with cytosolic calcium between 200 and 300 nM (**Figure 1C**). Within 10 min of addition of RWPF, cytosolic calcium levels of MCF-7 cells began to increase gradually as indicated by an increase in fluorescence (panels at 4−20 min, **Figure 1A**). The increase in cytosolic calcium levels varied between cells and was in the range of 150−400 nM corresponding to a 100−300% overall increase in calcium levels (**Figure 1C**). Some of these cells exhibited a cytosolic level of calcium that is higher than usually observed in excited cells (*20*). These elevations in cytosolic calcium levels indicate the earliest recorded response to polyphenol treatment in human cells and may be an initiating event in the development of cytotoxicity in MCF-7 cells. After 20 min of incubation with RWPF, the fluorescence of the cells drastically decreased (**Figure 1A,C**) indicating a decrease in cytosolic calcium levels. In contrast to this, the MCF-10A cells preloaded with Calcium Green-2 and treated similarly with RWPF did not show any of the responses that were characteristic to MCF-7 cells. Though the resting level of calcium in MCF-10A cells appeared to be slightly higher (90−150 nM) than that in MCF-7 cells, there was no increase in the cytosolic calcium levels of these normal cells in response to polyphenol treatment (**Figure 1B,D**).

Effect of RWPF on Calmodulin Activity and Levels. Calmodulin, the ubiquitous calcium-binding protein and regulator of enzymes and proteins is another component, the activity and levels of which may regulate the calcium second messenger function. To investigate this possibility, MCF-7 and MCF-10A cells were grown in synchrony, calmodulin was extracted by standard procedures, and its activity and levels were determined. Overall, CaM activity was found to be much lower in MCF-7 cells as compared to the MCF-10A cells (**Figure 2A,B**). As well, RWPF treatment did not cause any significant changes in CaM activity in MCF-7 cells except at 12 h post-treatment (**Figure 2A**). Also, there were no major changes in calmodulin activity in MCF-10A cells in response to RWPF treatment (**Figure 2B**). However, the activity profiles did not exactly reflect CaM expression levels within the cells. Even though calmodulin activity levels were low in MCF-7 cells, the calmodulin protein levels in MCF-7 cells were considerably higher as compared to the MCF-10A cells (**Figure 3A,B**). These results suggested that any differences in CaM activity or CaM protein levels were marginal between MCF-7 cells and MCF-10A cells.

Immunohistochemical Localization of Calmodulin. To further evaluate any potential differences in calmodulin levels between MCF-7 cells and MCF-10A cells and compare it with the results from activity estimation and Western blot analysis, subcellular localization of calmodulin was performed. Thin sections of cells were incubated with a monoclonal primary antibody raised against a conserved epitope of calmodulin that is distinct from other calcium binding proteins such as troponin C (Sigma Chemical Company, Technical Bulletin C 3545). Calmodulin was localized by goat anti-mouse IgGs coupled to 25 nm gold particles. Subcellular structural details such as the plasma membrane, internal membranes, nucleus, and nucleolus were visible even without any staining. The micrographs of untreated and RWPF-treated MCF-7 cells, 3 h and 12 h after treatment, are shown in **Figure 4A**. The cellular structure is retained in the control cells 3 h and 12 h after initiating the experiment. Calmodulin is localized as distinct dots (arrow) and is widely distributed, being present in the cytosol and the nucleus. Marked changes in the subcellular structure were distinctly noticeable within 1 h of treatment with the RWPF (data not shown) and became very distinct 3 h after polyphenol treatment (**Figure 4A**). There was extensive disruption of the internal membrane systems with large-scale vacuolation within the cytoplasm showing large areas devoid of any electron-dense material (**Figure 4A**, Vac). After 12 h of treatment, damage to the membranous structures were more dramatic, with the plasma membrane and the nuclear membrane showing gaps and the cytoplasm having numerous vesicular structures. Thus, polyphenol treatment of MCF-7 cells resulted in substantial damage to the membranes. Calmodulin showed equal amount of localization in treated and untreated MCF-7 cells, as evident from the number of gold particles in these cells (**Figure 4C**).

By contrast to MCF-7 cells, MCF-10A cells were resistant to any structural changes within the cell in response to treatment with RWPF. Micrographs of untreated and RWPF treated MCF-

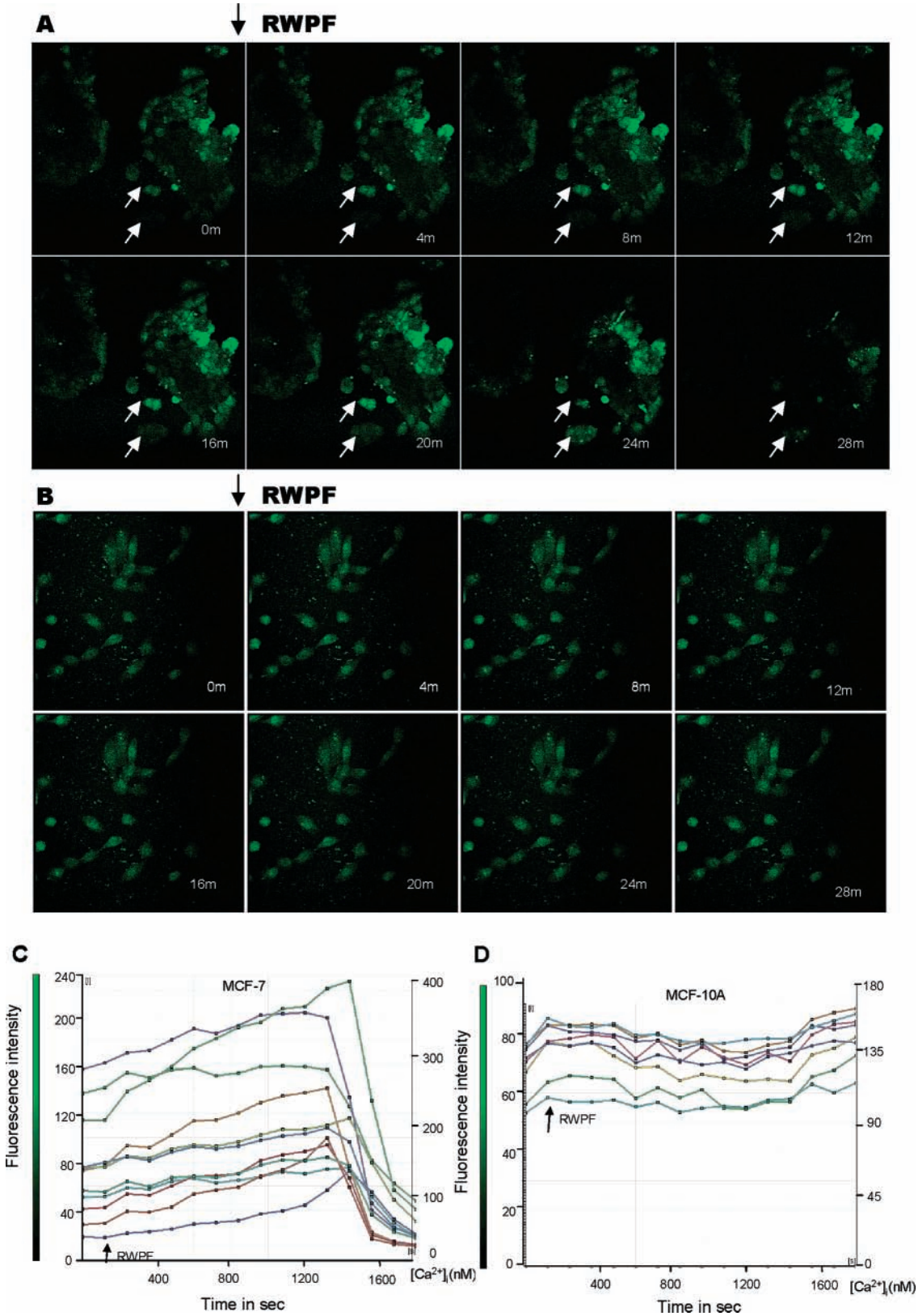

Figure 1. Intracellular Ca^{2+} changes after RWPF treatment. Intracellular Ca^{2+} levels were measured in live cells via confocal laser scanning microscopy using the Ca^{2+} indicator dye Calcium Green-2. MCF-7 and MCF-10A cells were loaded with Calcium Green-2. RWPF (50 μg) was added to the cells after basal images were recorded. Images of (**A**) MCF-7 and (**B**) MCF-10A cells collected every 4 min. The number in the lower right corner of each image represents the time (min) after addition of RWPF. These results are also displayed in graph form showing changes in fluorescence intensity and corresponding Ca^{2+} levels over time after RWPF treatment of (**C**) MCF-7 and (**D**) MCF-10A cells. Images were collected every 2 min for 30 min as indicated. Each line represents the change in Calcium Green-2 fluorescent emission of an individual cell over time. Calcium levels were calculated based on calibration using a standard of calcium at concentrations ranging from 0 to 400 nM. Increase in cytosolic calcium levels of MCF-7 cells after RWPF treatment varied between 100 and 300% of the basal levels. The data shown are representative of several separate experiments, all showing the same trend.

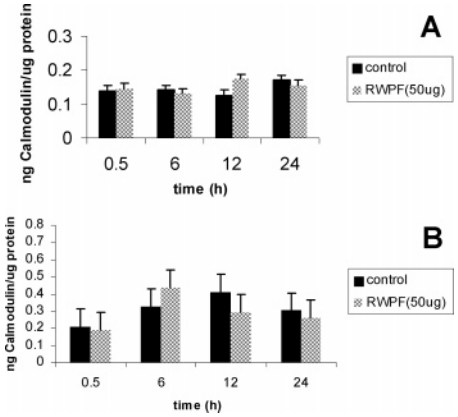

Figure 2. Measurement of calmodulin activity by cAMP phosphodiesterase assay. Calmodulin was purified by affinity chromatography from RWPF treated (50 μg) cell lysates of MCF-7 and MCF-10A cells, lyophilized, and measured in terms of stimulation of phosphodiesterase activity. (**A**) Calmodulin activity in MCF-7 cells. (**B**) Calmodulin activity in MCF-10A cells. The values are mean ± SE from three separate experiments. There were no statistically significant differences between treatment and control sets ($p < 0.5$) except in MCF-7 cells, at 12 h after treatment.

10A cells, 3 h and 12 h after treatment, are shown in **Figure 4B**. The cells showed characteristic ultrastructural features such as the nucleus, nucleolus, and internal membranes. The cytoplasm of MCF-10A cells also revealed vesicular structures, but after treatment with RWPF, the vesicles were much enlarged in size providing the appearance of pseudo-podia-like structures. The internal structure appears to be maintained well even after 12 h of incubation. The numerical distribution of gold particles in the cytoplasm and the nucleus of MCF-10A cells did not vary between untreated and treated cells 3 h and 12 h after treatment. As well, there were no major differences in the numerical distribution of gold particles between MCF-7 and MCF-10A cells (**Figure 4C**).

Effect of RWPF Treatment on Mitochondrial Membrane Potential. Results from ultrastructural studies (see previous section) suggested that RWPF induced rapid and deleterious changes in MCF-7 cells, noticeably in its membrane organization. Earlier studies in our lab using the live−dead cell viability staining kit also showed a decrease in cell size suggestive of a loss in membrane surface area in MCF-7 cells subjected to polyphenol treatment and were showing symptoms of the loss of viability (*16*). To determine whether mitochondrial dysfunction could be an early causative event in the induction of RWPF-mediated cytotoxicity, we exposed MCF-7 cells grown in serum-containing medium to 50 μg of RWPF for 1 h. Mitochondrial membrane potential was assessed by confocal laser scanning microscopy determination of JC-1 fluorescence. The membrane potential sensitive dye JC-1 exists as a monomer at a low mitochondrial membrane potential emitting green fluorescence. But, at a higher membrane potential, JC-1 forms red fluorescent "J-aggregates" in the mitochondria. Under normal physiological conditions both red and green fluorescence-emitting forms of JC-1 are noticeable within the cell, with a prevalence of the red fluorescent forms. The mitochondrial population of untreated MCF-7 and MCF-10A cells exhibited both the green fluorescent forms (low redox potential) and the red fluorescent forms (high redox potential) (**Figure 5A,B**, untreated). Treatment with RWPF resulted in a decrease in the red fluorescent forms of mitochondria in MCF-7 cells indicating a potential drop in mitochondrial membrane potential (ψ_m) (**Figure 5A**, lower panel). The drop in mitochondrial membrane potential could be a result of calcium dysregulation in the mitochondria, ATP depletion, or oxidative stress due to free radicals. On the other hand, there was no major shift in the mitochondrial population that emitted red fluorescence to those that emitted green fluorescence in MCF-10A cells subjected to RWPF treatment at similar concentrations (**Figure 5B**, lower panel).

To further determine whether caspase activation plays a role in the induction of RWPF-mediated cell death, the activity of caspase-8, which is an upstream initiator caspase that activates effector or executioner caspases, was monitored in MCF-7 cells treated with 50 μg/mL RWPF for 24 h. MCF-7 cells showed progressive increase in cell death between 5 and 24 h of treatment (*16*). No change in caspase-8 activity was observed in the reaction mixture monitored over a period of 30 min (data not shown). This suggests that the cell death induced by RWPF may be caused by mechanisms different from the typical apoptotic pathway. This contention was again supported by the analysis of DNA laddering in RWPF-treated MCF-7 cells. To characterize the mode of cell death induced by the wine polyphenols, we further analyzed the oligonucleosomal fragmentation of genomic DNA in MCF-7 cells. DNA ladder formation was examined by agarose gel electrophoresis in MCF-7 cells treated with 50 μg of RWPF. Results indicated

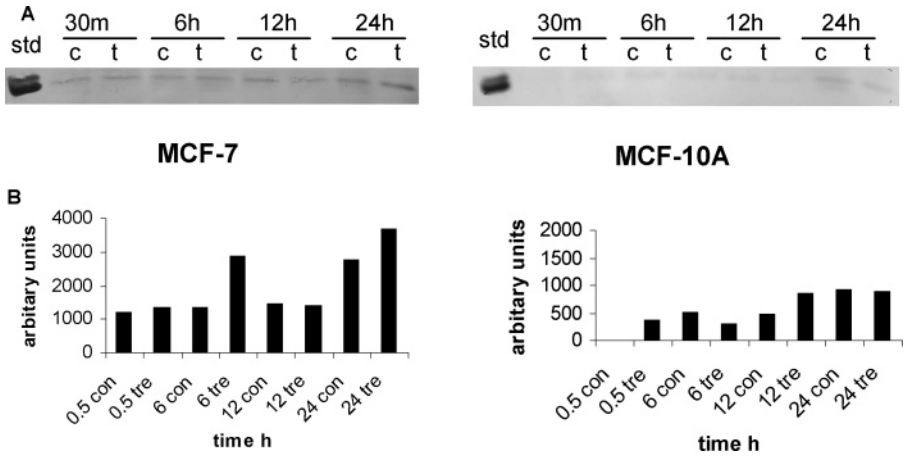

Figure 3. (**A**) Western blot analysis for calmodulin in MCF-7 and MCF10A cells, control (c) and treated (t) with RWPF (50 μg) for different time periods. (**B**) Densitometric scans of calmodulin band intensity levels in control and treated cells of MCF-7 and MCF10A at various time points. The data are representative of several experiments, showing the same trend. The band intensities did not show significant differences ($p < 0.05$) between treatment and control sets.

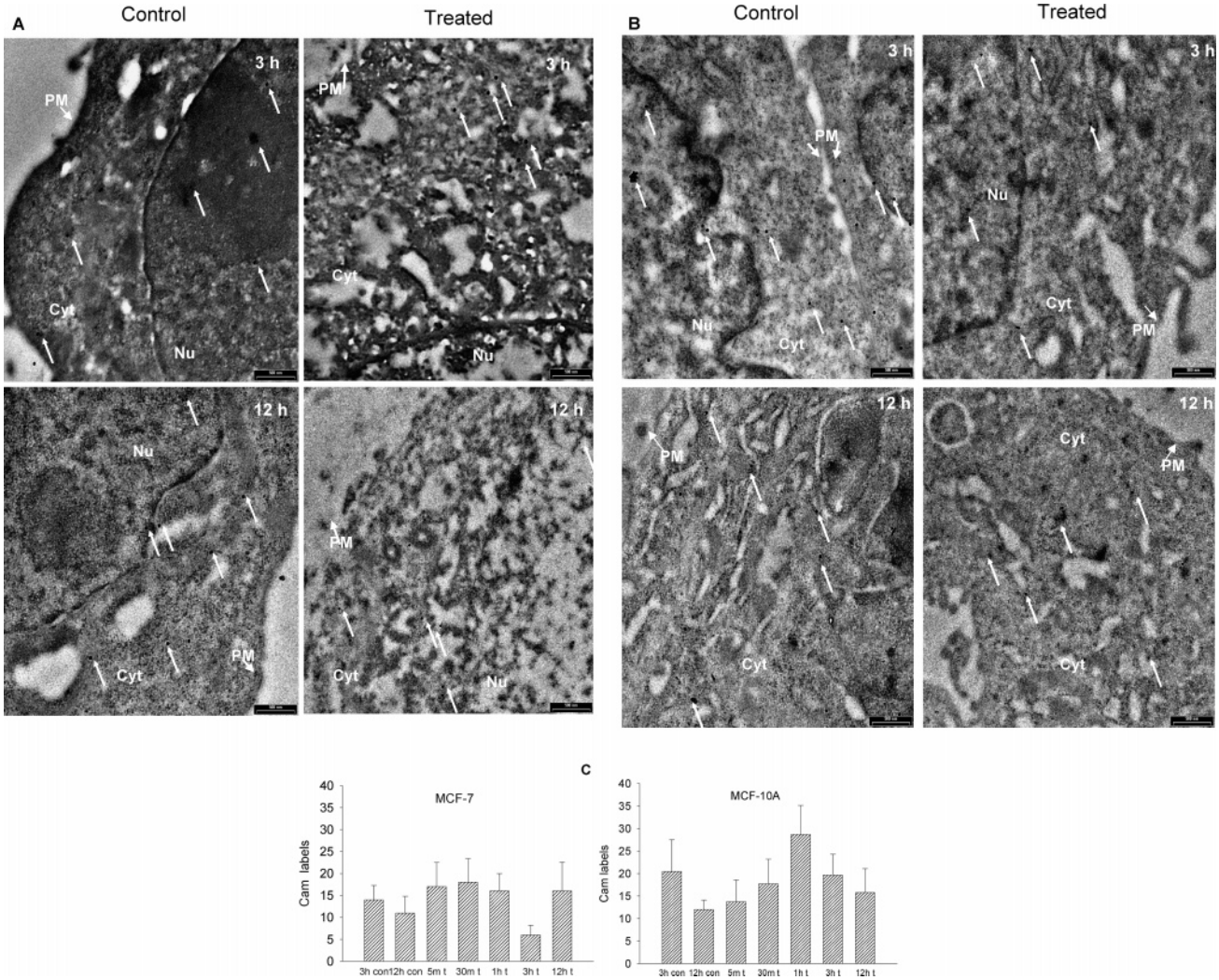

Figure 4. Transmission electron micrographs of MCF-7 and MCF-10A cells immunolabelled with monoclonal anti-calmodulin antibody and secondary antibody (goat-antimouse IgG) labeled with 20 nm gold particles. (**A**) Ultrastructure and immunolocalization of calmodulin in MCF-7 cells untreated (3 h, 12 h, left panel) and treated with 50 μg RWPF (3 h, 12 h, right panel). Calmodulin labeled with the gold appear as dark dots as shown by the arrows. Plasma membrane (PM), cytoplasm (Cy), and nucleus (Nu) are shown. Extensive vacuolation in the cytoplasm of treated MCF-7 cells are visible as early as 3 h (Vac). After 12 h of treatment, membrane integrity was severely disrupted, and the dissolution of cytoplasmic and nuclear membrane was apparent. (**B**) Ultrastructure and immunolocalization of calmodulin in MCF-10A cells untreated (3 h, 12 h, left panel) and treated (3 h, 12 h, right panel) with RWPF. Calmodulin bound to antibody–gold conjugates are shown by arrows. The plasma membrane (PM), cytoplasm (Cy) and nucleus (Nu) are shown. The figures are representative of several such cells showing similar structural features. The bar represents 500 nm. (**C**) Number of calmodulin labels detectable in MCF-7 and MCF-10A cells. The number of gold particles (mean ± SE) were counted in several cells (n = 8–10) that were untreated and subjected to RWPF for various time points. The number of gold particles between control and treated cells were not statistically significant ($p < 0.05$).

that wine polyphenols did not induce DNA fragmentation after 3, 6, 12, or 24 h of treatment (data not shown). These results suggested that a loss in mitochondrial membrane potential in MCF-7 cells treated with RWPF was followed by cell damage and death through a mechanism that was independent of caspase activation and did not follow the typical apoptotic pathway.

Determination of Lytic Compartments by Acridine Orange Staining. Results from the previous experiments including investigations on mitochondrial potential, DNA laddering, and electron micrographs indicated that the senescence of MCF-7 cells caused by RWPF treatment was neither typical of apoptosis nor that of necrosis. A characteristic response to the treatment in both MCF-7 and MCF-10A cells was the formation of membrane vesicles in the cytoplasm. In MCF-7 cells, these vesicles were small and numerous, whereas in MCF-10A cells, the vesicles that appeared to originate from the swelling of ER coalesced to form large vesicular structures, which later appeared to fuse with the plasma membrane (**Figure 4A,B**). Formation of acidic lytic compartments is a characteristic feature of the senescence process. Therefore, we tried to determine if cell death in MCF-7 cells involved the formation of acidic vesicular organelles. Acidic vacuoles in the cytoplasm can be localized by staining with acridine orange; acridine orange is a weak base, which gets trapped in acidic compartments when it becomes protonated and emits red fluorescence. In MCF-7 control and RWPF-treated cells (**Figure 6A**) as well as MCF 10A control and RWPF-treated cells (**Figure 6B**), the cytoplasm appeared green after staining with acridine orange (**Figure 6**, green). The cytoplasm of MCF-7 cells possessed a large number of tiny red fluorescent vesicles that gave an orange hue to the merge images (**Figure 6A**, merge). By contrast, the vesicles that emitted red fluorescence were few in untreated MCF-10A cells (**Figure 6**, red and merge). However, by contrast to MCF-7 cells, these vesicles in MCF-10A cells appeared to be much

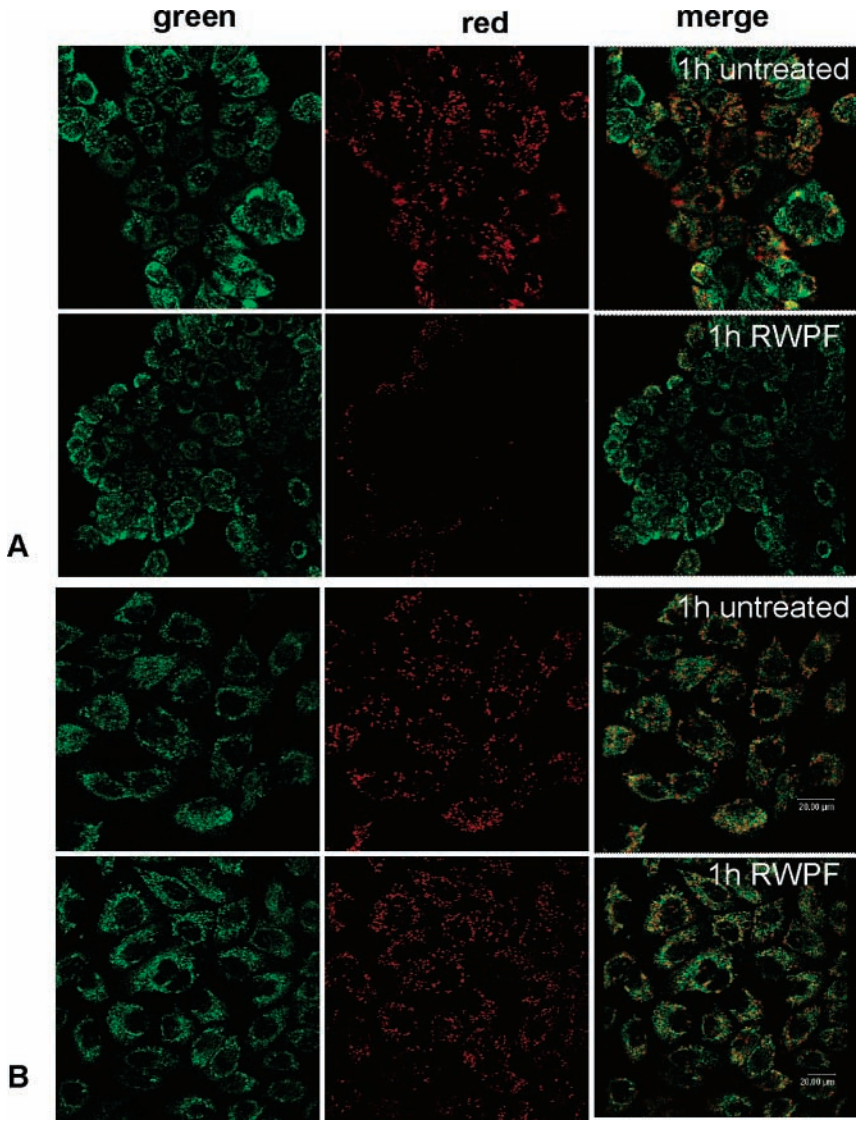

Figure 5. Evaluation of mitochondrial membrane potential ($\Delta\psi_m$) in untreated and RWPF-treated MCF-7 and MCF-10A cells by confocal laser scanning microscopy. The cells were loaded with 1 μM JC-1 in culture medium and incubated for 15 min; cells were washed and treated with 50 μg RWPF for 1 h. Green fluorescence was measured at 510 nm excitation/527 nm emission, and red fluorescence was measured at 585 nm excitation/590 nm emission. (**A**) Untreated and RWPF-treated MCF-7 cells. (**B**) Untreated and RWPF-treated MCF-10A cells. The data are representative of several experiments showing similar results.

larger. Interestingly, RWPF-treated MCF-10A cells appeared to possess a larger number of the red fluorescent vesicles (**Figure 6B**, red and merge). These vesicular structures were very similar to those seen during electron microscopy of MCF-10A cells (**Figure 4B**, Vac). Thus, in response to RWPF treatment, MCF-10A cells appear to form an increased number of vesicular structures that accumulate acridine orange. Whether this has any role in maintaining the cell integrity is not clear at this point.

Cell Cycle Arrest by Wine Polyphenols. To elucidate whether the alteration of cell cycle occurred following the addition of RWPF, the DNA content was measured by flow cytometry analysis. DNA histograms and the percentages of cells in each phase of the cell cycle are presented in **Figure 7**. Compared with the control MCF-7 cells, treatment with RWPF (50 μg/mL) resulted in a prominent increase in the G2/M population, showing an increase from 26.4% to 47.65%. In parallel with this, the proportion of cells in the S phase of RWPF-treated MCF-7 cells decreased drastically from 25.3 to 1.9% (**Figure 7A,B**). The proportion of MCF-7 cells in the G1 phase was nearly identical in both untreated and RWPF-treated sets (**Figure 7A,B**). This showed that red wine polyphenols induced a dramatic G2/M arrest in MCF-7 cells and a decrease in S-phase cells. By contrast, the MCF-10A cells showed no significant changes in the proportion of cells in G2/M or S-phase (**Figure 7A,B**) after RWPF treatment.

DISCUSSION

Conventional chemotherapy becomes ineffective when it results in severe side effects or cancer cells acquire multiple drug resistance. With increasing interest in alternative medicine and the need for nontoxic therapeutic approaches, research has recently been focused on natural components from the diet such as polyphenols, as these are effective against cancer cells and safe to the normal cells. Most of the previously published work on the chemopreventive action of polyphenols was related to their antioxidant properties (*21*). However, in the past decade, research on polyphenols has been focused on their non-antioxidant functions, specifically their ability to modulate signal

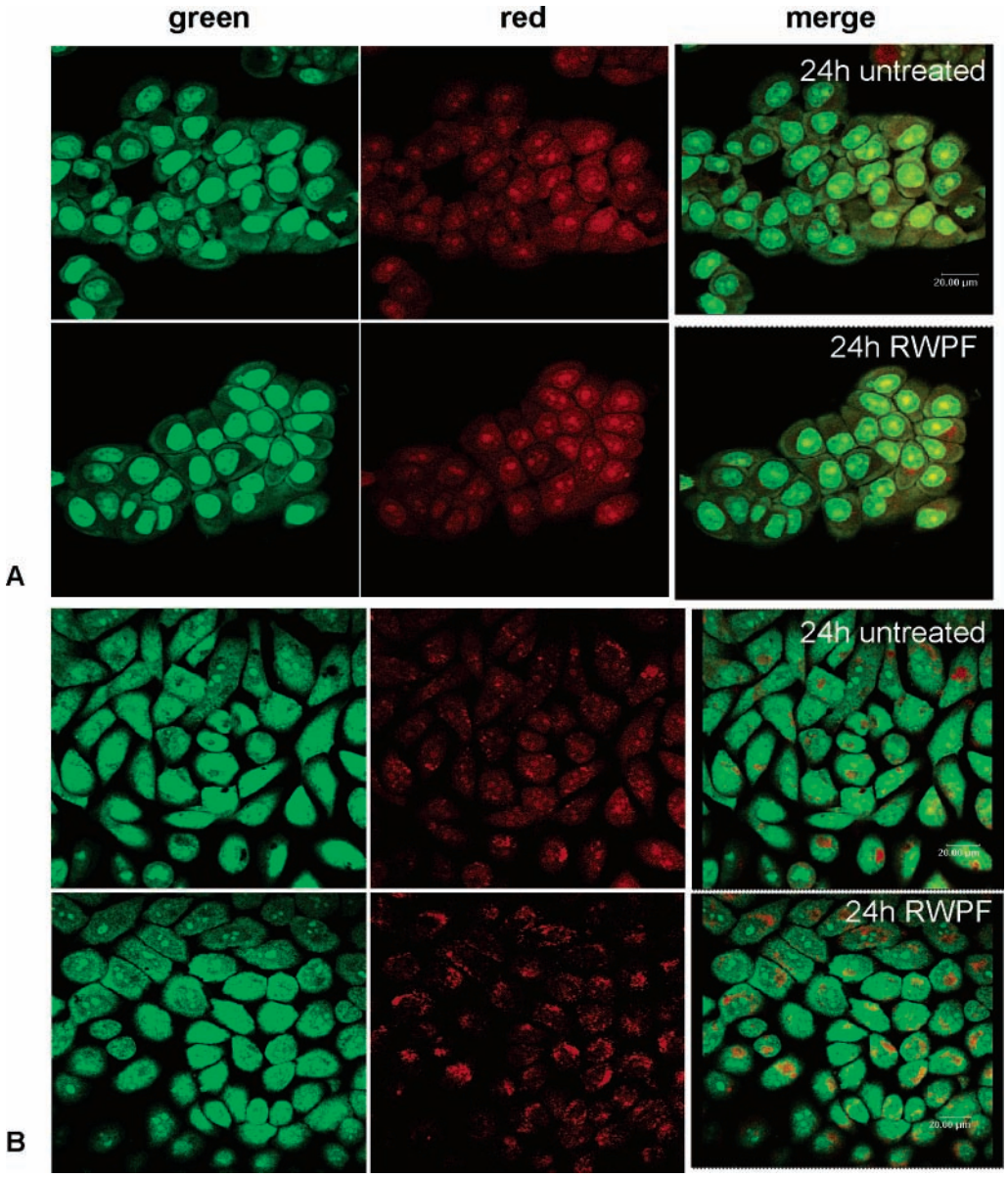

Figure 6. Fluorescence detection of acridine orange entrapment in vesicles of MCF-7 and MCF-10A cells, untreated and subjected to 50 μg RWPF treatment for 24 h. Cells were stained with 2.5 μg of acridine orange before visualizing by confocal laser scanning microscopy. The red and green images are shown as a merge in the extreme right panels. (**A**) Untreated and RWPF-treated MCF-7 cells. (**B**) Untreated and RWPF-treated MCF-10A cells. The data are representative of several experiments showing similar results.

transduction pathways. Several flavonoids in pure isolated forms have been shown to modulate signal transduction pathways in many ways that ultimately triggers cancer cell death due to apoptosis, necrosis or cell cycle arrest (*15, 22*).

In the present study, we have tested the hypothesis that RWPFs (that consist of a mixture of several flavonoid and non-flavonoid molecules in the food matrix) modulate the calcium signal transduction system in breast cancer cells and cause selective cytotoxicity in these cells. Cytosolic calcium levels are precisely controlled under physiological conditions and are usually in the low nanomolar range during resting conditions. In response to hormones or growth regulators, cytosolic calcium levels show a transient increase due to a controlled release from storage compartments such as the endoplasmic reticulum (*7, 8*) reaching high nanomolar levels. Calcium is pumped back into the storage compartments through ATP-dependent sequestration by the activity of calcium ATPases. Thus, if the calcium release/sequestration mechanisms were impaired in the MCF-7 cells, these cells are likely to maintain an elevated level of cytosolic calcium but at a level that does not cause cytotoxicity (*23*). An increase in cytosolic levels of calcium above the normally excited levels leads to cell death (*23*). Our findings revealed that there was a prolonged increase in the cytosolic calcium levels in MCF-7 cells in the range of 150−400 nM. This was initiated within 2−3 min of RWPF treatment and is quite distinct from the transient increase in cytosolic calcium elicited in response to hormones and agonists (*8*). Similar results have also been observed in bovine aortic endothelial cells subjected to polyphenolic components isolated from red wine, red wine powder (provinol), and delphinidin (*24*). Transient elevation in cytosolic calcium levels in the range of 100−200 nM was observed that on the average lasted for less than 100 s and activated signal transduction pathways leading to the production of nitric oxide, an inducer of vascular relaxation. By contrast to a transient increase, a sustained increase in calcium levels indicates an early event in the induction of a cellular death

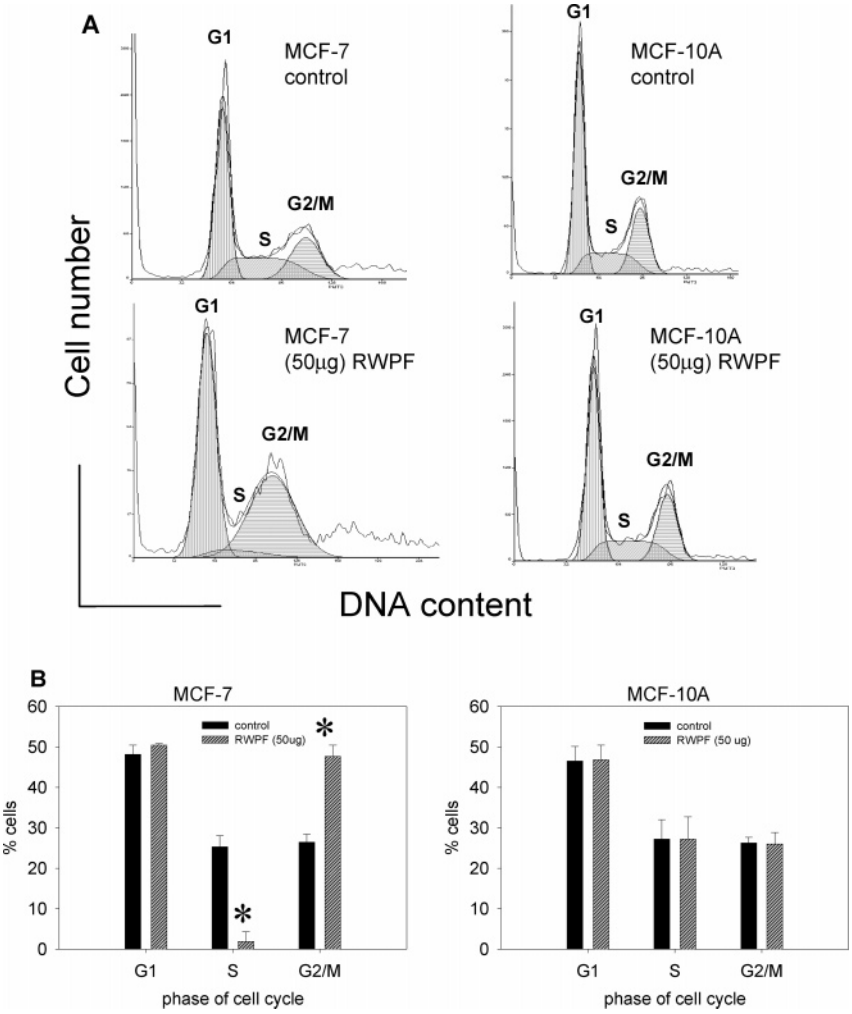

Figure 7. Effect of RWPF treatment on the cell cycle. Cell cycle profiles of MCF-7 and MCF-10A cells after treatment with 50 μg RWPF for 48 h by fluorescence-activated cell sorter (FACS) analysis. (**A**) Distribution of cells in G1,S and G2/M phases in MCF-7 and MCF-10A cells that are untreated and subjected to RWPF treatment. (**B**) Quantitative estimation of the percent of cells in G1,S and G2/M. MCF-7 cells showed a dramatic increase in G2/M phase cells from 26.4% to 47.6% indicating a G2/M block and a decrease in S phase cells from 25.3% to 1.9%. The values are mean ± SE from three independent evaluations. Statistical analysis was conducted using unpaired *t*-test, and significant differences at $p < 0.05$ vs the controls are marked by asterisks.

response. The results from our study are in agreement with other reports that have shown prolonged increases in cytosolic calcium levels to be associated with cytotoxicity (*25*). The sudden drop in calcium levels observed after 20 min of RWPF treatment could potentially be due to the activation of the Ca^{2+} uniporter by flavonoids as suggested in other studies (*26*), leading to an uptake of Ca^{2+} by the mitochondria or ER or a leakage of calcium ions from the cells due to a loss in membrane integrity.

Calmodulin is a major calcium-dependent regulatory protein, and an increase in cytosolic calcium is expected to lead to increased binding between calcium and calmodulin and subsequent activation of calcium−calmodulin-dependent enzymes. Overactivation of calcium−calmodulin complex has been implicated in carcinogenesis. Studies have shown that calmodulin is overexpressed in cancer cells as compared to their normal counterparts (*27*), and calmodulin antagonism has been perceived as an anti-tumor mechanism (*28*). However, evidence regarding the role of calmodulin in regulating cell death is complex. Dowd et al. (*29*) have shown that calmodulin expression is upregulated in glucocorticoid-mediated apoptosis of lymphocytes. Furuya and Issacs (*30*) have shown that mRNA expression of calmodulin increased 6−7-fold during the period of programmed death in prostatic glandular cells induced by castration. We found that calmodulin was overexpressed in MCF-7 breast cancer cells as compared to the normal MCF-10A cells, but changes in calmodulin activity were not obvious between untreated and RWPF-treated MCF-7 cells. This may be expected given that calmodulin is involved in regulating diverse cell functions from protein phosphorylation/dephosphorylation to cell proliferation. Changes in localization of CaM in RWPF-treated cells as compared to the untreated controls were also not evident as seen in immunogold-labeled cell micrographs using anti-CaM antibody. However, ultrastructural visualization of non-labeled specimens indicated that membrane structure and integrity were compromised in RWPF-treated MCF-7 cells, and this increased progressively with time. Thus, irrespective of changes in calmodulin levels and activity, it appears that RWPF-induced calcium release could have activated biochemical processes that in turn triggered changes in membrane structure and organization, causing senescence.

Attempts to characterize the senescence process led us to evaluate several other biochemical features downstream of calcium signalling. Mitochondria regulate several aspects of cell function such as energy production, redox status, biomolecular synthesis and metabolism, calcium signalling, and programmed cell death. A number of studies have been focused on

understanding the role of mitochondria in apoptotic signalling in cancer cells (*31*). Mitochondrial dysfunction could result in cell death or apoptosis through dysregulation in calcium homeostasis, ATP depletion, or oxidative stress (*32*). However, the link between calcium signalling, mitochondrial dysfunction, and cellular death is not fully understood. It is well-known that the maintenance of mitochondrial calcium homeostasis is dependent on mitochondrial membrane potential (*33*). Disruption of calcium homeostasis results in a loss of mitochondrial membrane potential. Our results show that changes in calcium signalling in MCF-7 cells treated with RWPF are followed by a loss of mitochondrial membrane potential. On the other hand, it is important to note that a drop in mitochondrial potential did not occur in MCF-10A cells since these cells did not show a dysregulation in calcium homeostasis.

Decrease in mitochondrial potential has been associated with apoptosis and cell cycle arrest in several studies (*34*, *35*). However, experiments to determine caspase activity and DNA laddering (apoptosis markers) in RWPF-treated MCF-7 cells did not support apoptosis as the mode of cell death. Accumulation of acidic vesicular structures is also an indication of programmed cell death by autophagy. However, in contrast to MCF-7 breast cancer cells, RWPF-treated MCF-10A cells showed a number of potentially acidic vesicular structures that accumulated acridine orange. Whether this plays a role in maintaining the cellular integrity of normal cells and increased sensitivity of cancer cells is not clear at this point.

At the cell cycle level, investigations with pure flavonoid compounds have shown that these compounds cause arrest of cancer cells at different stages of the cell cycle depending on their structure or the cell type on which they are acting. For example, quercetin blocks the cell cycle at the G1/S transition in gastric cancer cells and leukaemic cells (*36*), whereas it causes a G2/M block in breast and laryngeal cancer cell lines (*37*). Genistein induces both G1 and G2 blocks in BALB/c 3T3 fibroblasts or mouse melanoma cells (*38*). In a recent study, specific polyphenol fractions from cranberry have shown to induce apoptosis in several human breast cancer cell lines through a block in cell cycle progression (*39*). In this study, RWPF was observed to arrest cell cycle progression in MCF-7 cells at the G2/M phase that was evident by an increase in the percentage of G2/M population and a dramatic reduction in the S phase cells. In contrast to this, the cell cycle profile of MCF-10A cells was unchanged with polyphenol treatment.

Most of the investigations on the effect of polyphenols on cancer cell proliferation have been conducted with pure or isolated flavonoid compounds. This is one of a few studies where a complex mixture of polyphenols was used to treat the cells for evaluating cell survival and cell death. In this study, the effects observed are early responses to polyphenol treatment. The concentration of polyphenols we have used in this study (50 μg/mL) represents the IC_{50} for MCF-7 cells and may be in a higher range since, using an 80% fraction alone, an IC_{50} of 1−2 μg/mL was obtained (*16*). A continuation of the present study (Hakimuddin, Tiwari, Paliyath and Meckling, unpublished) showed that grape polyphenols given at 50 mg/kg body weight/day to athymic nude mice transplanted with the estrogen receptor negative MDA-MB-231 cells totally arrested the growth of the tumor. It has been reported that a plasma concentration of polyphenols in the range of 2.5 μg/mL is achievable after an intake of 100 mL of red wine (*40*). In another study subjects received 3.57 g of total anthocyanins in 150 mL of elderberry juice, and only a small proportion (<4 mg) was excreted in the urine after 5 h (*41*). Irrespective of the plasma concentrations achieved after the ingestion of anthocyanins or foods containing anthocyanins, it appears that physiological effects may be achievable at concentrations normally consumed (>2 g/day assuming a body weight of 50 kg). In summary, our findings reveal that red wine polyphenols show selective toxicity to MCF-7 breast cancer cells by affecting calcium homeostasis and calcium-dependent processes such as mitochondrial function and cell cycle progression. Thus, red wine polyphenols may exert a synergistic or additive action by modulating the function of multiple targets that are potentially activated in cancer cells as suggested by Liu et al. (*42*) with evidence from several epidemiological and laboratory studies. Altered signalling pathways in cancer cells need to be thoroughly explored in order to design new therapeutic strategies for preventing and treating malignant tumors. The results from this study argue for the role of dietary polyphenols as signalling molecules and provide useful directions to develop dietary preventive strategies and nutraceutical products that would target cancer cells with minimal toxic effects to normal cells. Potential therapies, combined with dietary interventions such as incorporation of wine polyphenols into the diet hold exciting possibilities for cancer treatment.

ACKNOWLEDGMENT

We are extremely grateful to Bob Harris, Electron Microscopy Centre, University of Guelph, for his help with the immunoelectron microscopy. We would also like to thank Dr. Michaela Strueder-Kypke, Department of Botany, University of Guelph, for her kind help and useful suggestions for conducting laser confocal scanning microscopy.

LITERATURE CITED

(1) Wingo, P. A.; Tong, T.; Bolden, S. Cancer statistics, 1995. *CA Cancer J. Clin.* **1995**, *45*, 8−30.
(2) Block, G.; Patterson, B.; Subar, A. Fruit, vegetables, and cancer prevention: a review of the epidemiologic evidence. *Nutr. Cancer* **1992**, *18*, 1−29.
(3) Longnecker, M. P. Alcoholic beverage consumption in relation to risk of breast cancer: meta-analysis and review. *Cancer Causes Control* **1994**, *5*, 73−82.
(4) Slattery, M. L.; O'Brien, E.; Mori, M. Disease heterogeneity: does it impact our ability to detect dietary associations with breast cancer? *Nutr. Cancer* **1995**, *24*, 213−220.
(5) Freedman, A. N.; Michalek, A. M.; Marshall, J. R.; et al. Familial and nutritional risk factors for p53 over expression in colorectal cancer. *Cancer Epidemiol., Biomarkers Prev.* **1996**, *5*, 285−291.
(6) Amundadottir, L. T.; Leder, P. Signal transduction pathways activated and required for mammary carcinogenesis in response to specific oncogenes. *Oncogene* **1998**, *16*, 737−746.
(7) Clapham, D. E. Calcium signalling. *Cell* **1995**, *80*, 259−268.
(8) Berridge, M. J.; Lipp, P.; Bootman, M. D. The versatility and universality of calcium signalling. *Nature* **2000**, *1*, 11−21.
(9) Lopez-Girona, A.; Colomer, J.; Pujol, M. J.; Bachs, O.; Agell, N. Calmodulin regulates DNA polymerase alpha activity during proliferative activation of NRK cells. *Biochem. Biophys. Res. Commun.* **1992**, *184*, 1517−1523.
(10) Rasmussen, C. D.; Means, A. R. Calmodulin is required for cell cycle progression during G1 and mitosis. *EMBO J.* **1989**, *8*, 73−82.
(11) Middleton, E.; Kandaswami, C.; Theoharides, T. C. The effects of plant flavonoids on mammalian cells: Implications for inflammation, heart disease and cancer. *Pharmacol. Rev.* **2000**, *52*, 673−751.
(12) Holmes-McNary, M.; Baldwin, A. S. Chemopreventive properties of trans-resveratrol are associated with inhibition of activation of 1 kappa B kinase. *Cancer Res.* **2000**, *60*, 3477−3483.

(13) Choi, S.; Singh, S. V. Bax and Bak are required for apoptosis induction by sulforaphane, a cruciferous vegetable-derived cancer chemopreventive agent. *Cancer Res.* **2005**, *65*, 2035−2043.
(14) Damianaki, A.; Bakogcorgou, E.; Kampa, M.; Notas, G.; Hatzoglou, A.; Panagiotou, S.; Gemetzi, C.; Kouroumalis, E.; Martin, P. M.; Castanas, E. Potent inhibitory action of red wine polyphenols on human breast cancer cells. *J. Cell. Biochem.* **2000**, *78*, 429−441.
(15) O'Prey, J.; Brown, J.; Fleming, J.; Harrison, P. R. Effects of dietary flavonoids on major signal transduction pathways in human epithelial cells. *Biochem. Pharmacol.* **2003**, *66*, 2075−2088.
(16) Hakimuddin, F.; Paliyath, G.; Meckling, K. Selective cytotoxicity of a red grape wine flavonoid fraction against MCF-7 cells. *Breast Cancer Res. Treat.* **2004**, *85*, 65−79.
(17) Paliyath, G.; Poovaiah, B. W. Calmodulin inhibitor in senescing apples and its physiological and pharmacological significance. *Proc. Natl. Acad. Sci. U.S.A.* **1984**, *81*, 2065−2069.
(18) Gopalakrishna, R.; Anderson, W. B. Ca^{2+}-induced hydrophobic site on calmodulin: application for purification of calmodulin by phenyl-sepharose affinity chromatography. *Biochem. Biophys. Res. Commun.* **1982**, *104*, 830−836.
(19) Bradford, M. M. A rapid and sensitive method for quantitation of microgram quantities of protein utilising the principle of protein-dye binding. *Anal. Biochem.* **1976**, *72*, 248−254.
(20) Chang, H.-T.; Huang, J.-K.; Wang, J.-L.; Cheng, J.-S.; Lee, K.-C.; Lo, Y.-K.; Liu, C.-P.; Chou, K.-J.; Chen, W.-C.; Su, W.; Law, Y.-P.; Jan, C.-R. Tamoxifen-induced increase in cytoplasmic free Ca^{2+} levels in human breast cancer cells. *Breast Cancer Res. Treat.* **2002**, *71*, 125−131.
(21) Heim, K. E.; Tagliaferro, A. R.; Bobilya, D. J. Flavonoid antioxidants: chemistry, metabolism and structure-activity relationships. *J. Nutr. Biochem.* **2002**, *13*, 572−584.
(22) Dross, R. V.; Xue, Y.; Knudson, A.; Pelling, J. C. Chemopreventive bioflavonoid apigenin modulates signal transduction pathways in keratinocyte and colon carcinoma cell lines. *J. Nutr.* **2003**, *133*, 3800S−3804S.
(23) Berridge, M. J.; Bootman, M. D.; Lipp, P. Calcium—a life and death signal. *Nature* **1998**, *395*, 645−648.
(24) Martin, S.; Andriambelosan, E.; Takeda, K.; Andriantsitohaina, R. Red wine polyphenols increase calcium in bovine aortic endothelial cells: a basis to elucidate signalling pathways leading to nitric oxide production. *Br. J. Pharmacol.* **2002**, *135*, 1579−1587.
(25) Zhang, W.; Coldwell, W. T.; Song, H.; Takano, T.; Lin, J.; Nedergaard, H. C. Tamoxifen-induced enhancement of calcium signalling in glioma and MCF-7 breast cancer cells. *Cancer Res.* **2000**, *60*, 5395−5400.
(26) Montero, M.; Lobaton, C. D.; Hernandez-Sanmiguel, E.; et al. Direct activation of the mitochondrial calcium uniporter by natural plant flavonoids. *Biochem. J.* **2004**, *384*, 19−24.
(27) Takemoto, D.; Jilka, C. Increased content of calmodulin in human leukemia cells. *Leuk. Res.* **1983**, *7*, 97−100.
(28) Jacobs, E.; Bulpitt, P. C.; Coutts, I. G.; Robertson, I. F. New calmodulin antagonists inhibit in vitro growth of human breast cancer cell lines independent of their estrogen receptor status. *Anticancer Drugs* **2000**, *11*, 63−68.
(29) Dowd, D. R.; MacDonald, P. N.; Komm, B. S.; Haussler, M. R.; Miesfeld, R. Evidence for early induction of calmodulin gene expression in lymphocytes undergoing glucocorticoid-mediated apoptosis. *J. Biol. Chem.* **1991**, *266*, 18423−18426.
(30) Furuya, Y.; John, T. I. Differential gene regulation during programmed death (apoptosis) versus proliferation of prostatic glandular cells induced by androgen manipulation. *Endocrinology* **1993**, *133*, 2660−2666.
(31) Green, D. R.; Reed, J. C. Mitochondria and apoptosis. *Science* **1998**, *281*, 1309−1312.
(32) De Lisa, F.; Bernardi, P. Mitochondrial function as a determinant of recovery or death in cell response to injury. *Mol. Cell Biochem.* **1998**, *184*, 379−391.
(33) Richter, C. Pro-oxidants and mitochondrial Ca^{2+}: their relationship to apoptosis and oncogenesis. *FEBS Lett.* **1993**, *325*, 104−107.
(34) Heerdt, B. G.; Houston, M. A.; Augenlicht, L. H. Short-chain fatty acid-initiated cell cycle arrest and apoptosis of colonic epithelial cells is linked to mitochondrial function. *Cell Growth Differ.* **1997**, *8*, 523−532.
(35) Kothan, S.; Dechsupa, S.; Leger, G.; Moretti, T. L.; Vergote, J.; Mankhetkorn, S. Spontaneous MMP change during apoptotic induction by quercetin in K562 and K562/adr cells. *Can. J. Physiol. Pharmacol.* **2004**, *82*, 1084−1090.
(36) Yoshida, M.; Yamamoto, M.; Nikaido, T. Quercetin arrests human leukemic T-cells in late G1 phase of the cell cycle. *Cancer Res.* **1992**, *52*, 6676−6681.
(37) Ferrandina, G.; Almadori, G.; Maggiano, N.; Lanza, P.; Ferlini, C.; Cattani, P.; Piantelli, M.; Scambia, G.; Ranelletti, F. O. Growth inhibitory effect of tamoxifen and quercetin and presence of type II estrogen binding sites in human laryngeal cancer cell lines and primary laryngeal tumors. *Int. J. Cancer* **1998**, *77*, 747−754.
(38) Kuzumaki, T.; Kobayashi, T.; Ishikawa, K. Genistein induces $p21^{Cip1/WAFI}$ expression and blocks the G1 to S phase transition in mouse fibroblast and melanoma cells. *Biochem. Biophys. Res. Commun.* **1998**, *251*, 291−295.
(39) Ferguson, P. J.; Kurowska, E.; Freeman, D. J.; Chambers, A. F.; Koropatnick, D. J. A flavonoid fraction from cranberry extract inhibits proliferation of human tumor cell lines. *J. Nutr.* **2004**, *134*, 1529−1535.
(40) Duthie, G. G.; Pedersen, M. W.; Gardner, R. T.; Morrice, P. C.; Jenkinson, A. M.; McPhail, D. B.; Steele, G. M. The effect of whisky and wine consumption on total phenol content and antioxidant capacity of plasma from healthy volunteers. *Eur. J. Clin. Nutr.* **1998**, *52*, 733−736.
(41) Bitsch, R.; Netzel, M.; Sonntag, S.; Strass, G.; Frank, T.; Bitsch, I. Urinary excretion of cyanidin glucosides and glucuronides in healthy humans after elderberry juice ingestion. *J. Biomed. Biotechnol.* **2004**, *5*, 343−345.
(42) Liu, R. H. Potential synergy of phytochemicals in cancer prevention. Mechanism of action. *J. Nutr.* **2004**, *134*, 3479S−3485S.

Received for review March 24, 2006. Revised manuscript received July 19, 2006. Accepted August 2, 2006. This study was supported by financial assistance from the Breast Cancer Society of Canada and the Food System Biotechnology Centre, University of Guelph.

JF060834M